

Corrosion of diffusion zinc coatings in sodium chloride solutions

Alexander I. Biryukov^a, Dmitry A. Zakharyevich^a, Tatyana V. Batmanova^{a*} ,
Rashit G. Galin^b, Maksim N. Ulyanov^a, Vladimir E. Zhivulin^c 

a: Chelyabinsk State University, Chelyabinsk 454001, Russia

b: Vika-Gal LTD, Chelyabinsk 454087, Russia

c: South Ural State University, Chelyabinsk 454080, Russia

* Corresponding author: batmanovatt@gmail.com

This paper belongs to a Regular Issue.

© 2022, the Authors. This article is published in open access under the terms and conditions of the Creative Commons Attribution (CC BY) license (<http://creativecommons.org/licenses/by/4.0/>).



Abstract

Diffusion galvanizing is widely used in the pipe industry for coating the threaded surface of pipe couplings and protecting water pipelines, gas pipelines, and other metal products. Diffusion coatings have a number of advantages over other types of zinc coatings. In this work, electrochemical and gravimetric methods were used to study the corrosion behavior of diffusion zinc coatings in sodium chloride solutions. The corrosion rate depends non-linearly on the thickness of the coating. At the initial stages, the corrosion rate of coatings depends on the structure of the phases on the surface, and with an increase in the holding time, the corrosion rate depends to a greater extent on the properties of the products formed during the corrosion process. The films of corrosion products of diffusion zinc coatings consist of zinc oxide/hydroxide and basic zinc salts, while the composition of the film changes with increasing coating thickness.

Keywords

corrosion
sherardizing
zinc
coatings

Received: 05.10.22

Revised: 10.11.22

Accepted: 11.11.22

Available online: 18.11.22

1. Introduction

Zinc coating is one of the most popular methods of protecting steel products from corrosion. Galvanic zinc coatings and the so-called "hot" zinc coatings are widely used in industry. These coatings are obtained by immersing steel products in a zinc melt. They differ in the chemical and phase composition, besides the method of application. Galvanic zinc coatings are practically pure zinc and are uniform in thickness. The coatings obtained from the melt consist of iron-zinc phases, which are distributed layer by layer, in accordance with the phase diagram of Zn-Fe [1]. According to the diagram, zinc and iron can form the following phases: α -; Γ -; δ -; ζ - and η -phase, in the order of increasing zinc concentration [1]. The composition of "hot" zinc coatings includes η - and ζ -phases with a zinc concentration of 95.0–96.0 wt.% [1, 2]. The corrosion behavior of such coatings has been studied by various authors [3–6] and is often interpreted on the basis of the corrosion mechanism of pure zinc [7–11].

The sherardizing method involves heating the steel products in mixtures based on zinc powders. The advantages of this approach are the possibility of obtaining coatings with desired properties, high productivity, minimal production waste and a low load on the environment.

Diffusion zinc coatings consist of iron-zinc phases, but their structure is dominated by a phase with a lower zinc content, the δ -phase (88.5–93.0 wt.%). A few works were devoted to the study of corrosion of diffusion zinc coatings [12–14].

Galín [15] developed a sherardizing technology using saturating powder mixtures with nanostructured zinc oxide. This technology is used now at the enterprises of JSC "PNTZ" and PJSC "SinTZ" for applying diffusion zinc coating on the threaded surface of tubing couplings and at other enterprises for galvanizing metal products. The technology makes it possible to obtain coatings consisting of predominantly single-phase layers of iron-zinc phases of relatively large thickness. The work [16] provides the data on the mechanical properties of the coatings, their hardness and corrosion under operating conditions. The purpose of this work is to study the corrosion behavior of diffusion zinc coatings using various laboratory corrosion test methods.

2. Materials and methods

Diffusion zinc coatings were applied to steel discs (steel 45) with a diameter of 32.0 mm and a thickness of 2.5 mm. The galvanizing temperature was 450 °C, the duration was from 1 to 4 hours. The saturating mixture contained

zinc particles with nanostructured oxide on the surface [15–18], which is a feature of the proprietary technology. The galvanizing technique is described in [15–18]. The resulting coatings have a dark gray color and a uniform appearance. The thickness of the coatings was determined with a magnetic thickness gauge. The samples with a thickness of 20 to 80 μm were used.

The corrosive medium in all studies was a 3 wt.% sodium chloride solution. It was prepared by dissolving weighed portions of a chemically pure grade reagent in distilled water.

The determination of the corrosion rate of the samples by the gravimetric method was carried out at room temperature, and the exposure time was 30 days. The geometric parameters of the samples were measured with an accuracy of 0.1 cm and weighed before and after testing with an accuracy of 0.0001 g. The corrosion products were removed mechanically after exposure. Based on the results of determining the area and weight loss, the corrosion rate was calculated as $\text{g}\cdot\text{m}^{-2}\cdot\text{hour}^{-1}$.

A flat corrosion cell was used to measure electrode potentials and polarization curves. A silver chloride electrode was used as a reference electrode (the potentials were recalculated to a standard hydrogen scale), and a graphite electrode served as an auxiliary one. The polarization curves were recorded after measuring the stationary potential, after 1 hour exposure in a corrosive environment. The polarization curves were obtained in the potential range from (-1.3) to (+0.2) V (SHE) with a sweep rate of $5\text{ mV}\cdot\text{s}^{-1}$. The curves were used to estimate the corrosion current density. The corrosion current density of the coatings under study was estimated from the point of intersection of the linear sections of the anodic and cathodic curves. The time dependences of the potential were obtained in the same clamping cell using a silver chloride reference electrode. The measurements were carried out for 60 minutes, until stationary values were established.

Corrosion products of diffusion zinc coatings were characterized using by X-ray phase analysis (DRON-3, $\text{Cu K}\alpha$) and scanning electron microscopy (Jeol JSM7001F microscope with an Oxford INCA X-max 80 energy dispersive spectrometer for X-ray spectral microanalysis).

3. Results and Discussion

In the previous works [17–19], the relationship between the coating thickness, phase and chemical composition of the surface layers is described in detail. The δ -phase (FeZn_{7-10}) is present on the surface of the coatings with a thickness of 10 to 40 μm , and for the coatings with a thickness of 50 to 80 μm the ζ -phase (FeZn_{13}) appears on the surface. The proportion of ζ -phase increases with the thickness of the coating. The corrosion behavior of diffusion zinc coatings was compared with samples of pure zinc, imitating galvanic zinc coatings and samples of a substrate made of steel 45.

3.1. Stationary potentials

Figure 1 shows a time dependence of the electrode potential of a coating. The potential shifts over time to the negative region by 90 mV. This is apparently due to the corrosion of the coating and the formation of a film of corrosion products. At the initial stage of the corrosion process, the film is inhomogeneous and does not protect the coating, since otherwise the electrode potential would be refined. Stationary potentials of different samples were compared (Table 1). Steel has the most positive potential, and zinc has the most negative potential. Their potentials differ by 300 mV, which with a small error corresponds to the difference between the standard electrode potentials of zinc and iron.

The stationary potentials of the coatings are in the range of -0.6 to -0.8 V (SHE). As the thickness increases, the electrode potential of the coating shifts to the negative region. This is due to the fact that with increasing thickness the concentration of zinc in the surface layer increases. Zinc has a more negative potential and, consequently, the coating potential also becomes more negative. No extremum is observed in the series of potentials.

3.2. Polarization curves

Figure 2 shows the polarization curves of the diffusion zinc coatings of various thicknesses. It can be seen that the coating with a minimum thickness of 10 μm has a more positive stationary potential, which can be explained by a relatively high concentration of iron. The electrode potentials of other coatings are in the range from -0.6 to -0.8 V (SHE), which corresponds to the distribution of stationary potentials of the coatings.

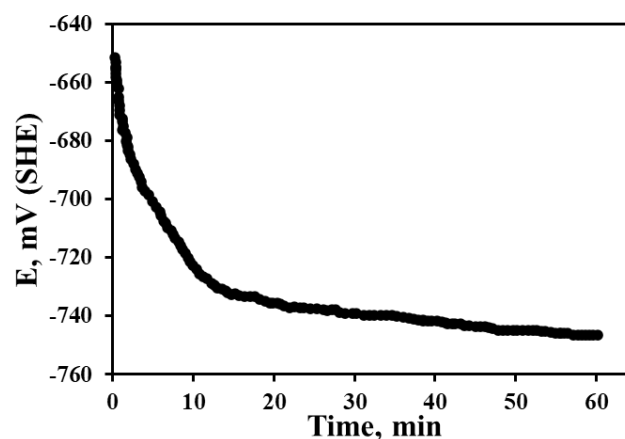


Figure 1 Dependence of E on τ for a zinc coating (50 μm).

Table 1 Stationary potentials of the samples.

| Sample / thickness, μm | E , mV (SHE) |
|-----------------------------------|----------------|
| Steel 45 | - 403 |
| Zinc coating /10 μm | - 600 |
| Zinc coating /20 μm | - 700 |
| Zinc coating /40 μm | - 738 |
| Zinc coating /80 μm | - 758 |
| Zinc | - 803 |

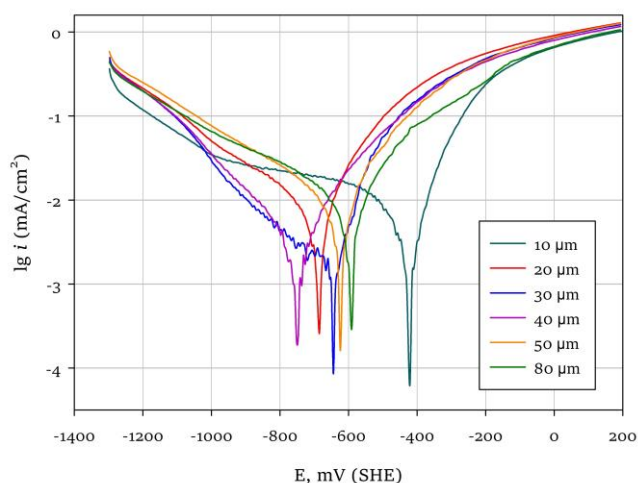


Figure 2 Polarization curves of diffusion zinc coatings of various thicknesses.

However, in this case, no strict dependence of the potential values is observed on the coating thickness. The anodic polarization curves do not have any inflection points, and the oxidation current increases uniformly as the potential is shifted. On the cathodic polarization curve of the 10 μm thick sample, a small current area is observed between the potentials -0.6 V and -1.0 V (SHE). This shape of the cathode curve corresponds to a slow diffusion of oxygen to the electrode surface. On the cathode curves of the remaining coatings, this section is not pronounced.

A nonlinear dependence of the corrosion current on the thickness is observed for the diffusion zinc coatings (Table 2). The samples of diffusion zinc coatings with a thickness of 30–40 μm have the minimum value of the corrosion current. In the previous works [19, 20], a minimum of the corrosion rate was also observed for the coatings on the surface of which the δ -phase was present, the composition of which approximately corresponds to the middle of the region of its existence in the Fe-Zn phase diagram.

The authors [19, 20] explained this by the structural features of the δ -phase, in particular, by the minimum number of relatively isolated zinc atoms in the structure, with the composition of the δ -phase corresponding to the observed minimum of the corrosion current. With an increase in thickness over 40 μm , which corresponds to the transition from the δ -phase to the ζ -phase, the corrosion current doubles compared to the coatings predominantly consisting of the δ -phase. The corrosion current increases to a lesser extent with a decrease in the thickness of the coatings, which can be associated with an increase in the concentration of iron in the surface layers.

3.3. Gravimetric tests

Figure 3 shows the dependence of the gravimetric corrosion rate of coatings on their thickness. The corrosion rate of steel 45 (the reference data according to [21]) is two times higher than the corrosion rate of zinc, and the corrosion rate of the coatings is in the range of 0.02 – 0.03 $\text{g}\cdot\text{m}^{-2}\cdot\text{h}^{-1}$ regardless of the thickness. When

passing from coatings with the δ -phase on the surface to coatings with the ζ -phase, a slight increase is observed in the corrosion rate, which may be associated with disturbances in the phase composition of the surface layers.

The gravimetric method also gives a nonlinear dependence of the corrosion rate on thickness, although the spread is less than that observed for the initial corrosion stage. The coatings that are in the middle of the studied thickness range have the maximum corrosion rate. This dependence differs from that obtained when assessing the corrosion current, where the coatings with a thickness of 30–40 μm had a minimum corrosion rate.

It should be noted that when recording the polarization curves, the exposure of the coatings in a corrosive environment did not exceed 1 hour, while, in the gravimetric studies, the exposure was 720 hours. Corrosion formed on the coatings during the long exposure.

3.4. Corrosion products

Figure 4 shows the diffraction patterns of the diffusion zinc coatings of different thicknesses after exposure for 720 hours in a 3% NaCl solution. The compositions of the corrosion products are similar, the films contain zinc oxide/hydroxide $\text{ZnO}/\text{Zn}(\text{OH})_2$ as well basic zinc salts. These include basic zinc chloride (simoncolleite) $\text{Zn}_5\text{Cl}_2(\text{OH})_8\cdot\text{H}_2\text{O}$ and basic zinc carbonate (hydrozincite) $\text{Zn}_5(\text{OH})_6(\text{CO}_3)_2$. Thus, the films of corrosion products are mixtures of zinc compounds with different ability to protect the metal from corrosion. With an increase in the thickness of the coating, the intensity of the peaks corresponding to zinc oxide/hydroxide increases, while the intensity of the peaks of simoncolleite and hydrozincite decreases.

Table 2 Corrosion currents of the investigated coatings in 3% NaCl solution.

| Thickness, μm | $i_{\text{corr}}\cdot 10^{-3}$, mA/cm^2 |
|--------------------------|--|
| 10 | 2,5 |
| 20 | 3,1 |
| 30 | 1,3 |
| 40 | 1,4 |
| 55 | 3,4 |
| 80 | 3,4 |

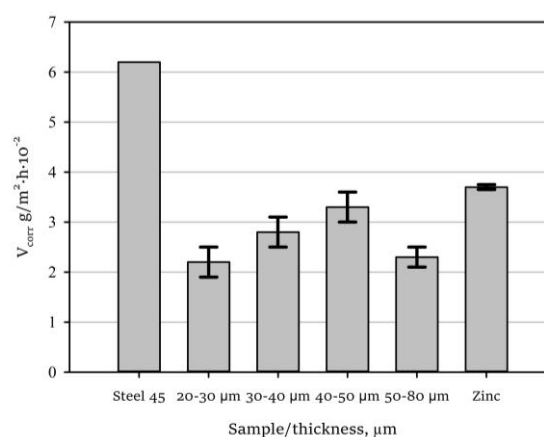


Figure 3 Corrosion rate of coatings, steel and zinc.

Figure 5 shows electron microscopic images of a transverse section of a coating (thickness 50 μm) after 720 hours exposition in 3% sodium chloride. The corrosion products (dark-gray area at the top part of Figure 5) uniformly cover the remaining coating and fill cracks and defects. Thus, the products of corrosion prevent further contact of the corrosive medium with the coating.

According to the X-ray microanalysis data, the corrosion products in cracks have the following chemical composition (at.%): O - 41.75; Cl - 9.55; Fe - 3.65; Zn - 45.05. The concentration of chemical elements satisfactorily corresponds to simonkolleite, which is confirmed by the X-ray phase analysis.

3.5. Discussion

Zinc corrosion is usually represented as the work of localized anode and cathode sites. Oxidation occurs at the anode sites:



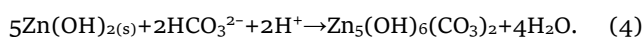
and oxygen reduction - at the cathode sites:



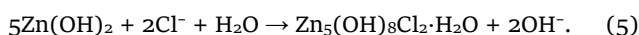
The accumulation of Zn^{2+} and OH^- leads to the formation of amorphous zinc hydroxide:



which, in turn, can be converted depending on pH to zinc oxide ZnO or crystalline forms of zinc hydroxide $\text{Zn}(\text{OH})_2$. These compounds exhibit semiconductor properties and poorly protect the metal from corrosion. If carbonate ions CO_3^{2-} or hydrocarbonate ions HCO_3^- are present in the solution, basic zinc carbonate $\text{Zn}(\text{CO}_3)_2(\text{OH})_6$ can be formed, for example, by the reaction [22,23]:



In solutions with a high content of chloride ions Cl^- , basic zinc chloride is formed $\text{Zn}_5\text{Cl}_2(\text{OH})_8 \cdot \text{H}_2\text{O}$ [22, 23]:



The literature describes various mechanisms for the formation of basic salts during the zinc corrosion. These compounds are known to form insoluble, poorly conductive films that are capable of slowing down the corrosion of zinc. However, the formation of such compounds takes some time [22, 23].

A feature of the corrosion of iron-zinc coatings FeZn and zinc alloys in general is the selective dissolution of zinc as a more electronegative metal. In a number of works [24, 25], it is noted that selective dissolution can have a positive effect on the anticorrosion properties of a film of corrosion products, in particular, due to the formation of a microheterogeneous rough surface, which is convenient for the nucleation of numerous crystallization centers, or due to the enrichment of the film with a more noble metal.

Thus, at the beginning of corrosion, with minimal exposure to the environment, the corrosion characteristics of

coatings are affected by the structure and phase composition of the surface layers. At this moment, there are no films of corrosion products on the surface of the coatings. The dependences of the corrosion current on the coating thickness at this stage can be explained by the structural and phase inhomogeneity of surface coatings of various thicknesses [19, 20].

With an increase in the exposure time, films of corrosion products have a greater effect on the corrosion rate. So, a loose layer of iron hydroxides is formed on the steel, which has low adhesion to the metal base. Such a layer of corrosion products poorly protects the sample from contact with an aggressive environment, so the corrosion rate of steel is the highest.

As shown by the authors of [26], in the presence of chloride ions on the surface of iron-zinc coatings, the formation of basic zinc salts occurs faster than on the surface of pure zinc. This explains the lower gravimetric corrosion rate of diffusion zinc coatings compared to pure zinc.

At the same time, when analyzing films of corrosion products, it can be seen that they are mixtures of various zinc compounds, both zinc oxide and basic salts. These compounds have different ability to inhibit the corrosion process. Increasing the concentration of zinc oxide/hydroxide in the film leads to an increase in the corrosion rate of the coatings.

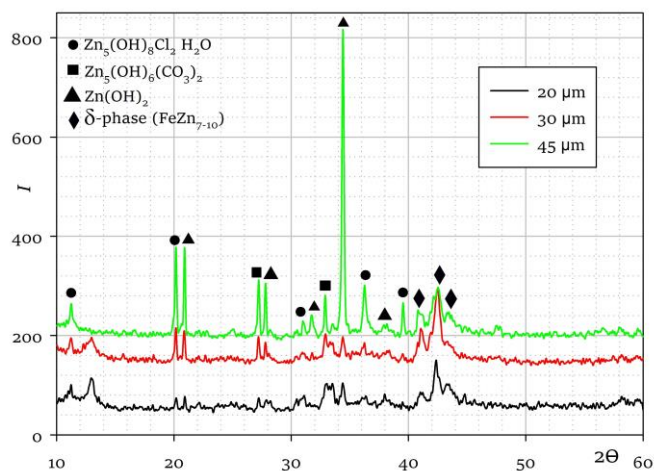


Figure 4 Diffraction patterns of corrosion products.

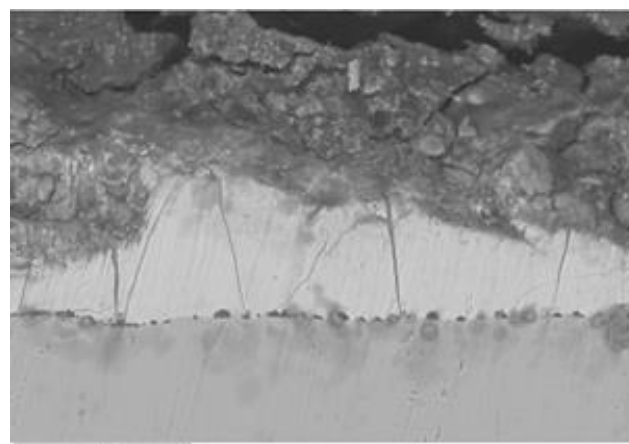


Figure 5 Cross section of coating after corrosion in 3% NaCl.

The question of the chemical or structural state of iron in corrosion products that provide the best long-term protection in a corrosive environment requires separate consideration. Some authors made assumptions about the reasons for the positive effect of iron on the protective ability of zinc corrosion products. In [24], the authors point to the formation of a dense deposit, which slows down the ionic conductivity. It was shown in [25] that a film of corrosion products with 7 wt.% Fe suppresses the oxygen reduction reaction due to its low electrical conductivity. In addition, in [27, 28], it was assumed that the effect of iron is reduced to the amorphization of the deposit of corrosion products, an increase in its compactness and a decrease in porosity.

4. Conclusions

The corrosion rate of diffusion zinc coatings depends non-linearly on the thickness, while on average it is two times less than the corrosion rate of steel and one and a half times less than the corrosion rate of zinc. At the initial stages, the corrosion rate of the coatings is influenced by the structure and phase composition of the surface layers of the coating. With an increase in the exposure time, the corrosion rate of the coating depends to a greater extent on the properties and composition of the film of corrosion products. The films of corrosion products of the diffusion zinc coatings consist of zinc oxide and basic zinc salts, while the composition of the films changes with increasing coating thickness.

Supplementary materials

No supplementary materials are available.

Funding

The research was funded by Russian Foundation for Basic Research and Chelyabinsk Region (project no. 20-43-740026), <https://kias.rfbr.ru/>.



Acknowledgments

None.

Author contributions

Conceptualization: B.A.I., B.T.V., Z.D.A., R.G.G.

Data curation: B.A.I.

Formal Analysis: B.A.I., Z.D.A., B.T.V.

Funding acquisition: B.A.I., Z.D.A., R.G.G.

Investigation: B.A.I., Z.D.A., B.T.V., M.N.U., V.E.Z.

Methodology: B.A.I., B.T.V., R.G.G.

Project administration: B.A.I., Z.D.A.

Resources: B.A.I., Z.D.A., B.T.V., R.G.G., M.N.U., V.E.Z.

Software: Z.D.A., B.T.V.

Supervision: B.T.V.

Validation: B.A.I., B.T.V.

Visualization: B.A.I., Z.D.A., B.T.V., V.E.Z.

Writing –original draft: B.A.I., B.T.V.

Writing –review & editing: B.A.I., Z.D.A.

Conflict of interest

The authors declare no conflict of interest.

Additional information

Author IDs:

Alexander I. Biryukov, Scopus ID [57190129477](https://orcid.org/0000-0001-5719-0129);

Tatyana V. Batmanova, Scopus ID [57208816951](https://orcid.org/0000-0001-5720-8816);

Dmitry A. Zakharyevich, Scopus ID [6507370493](https://orcid.org/0000-0001-6507-3704);

Maksim N. Ulyanov, Scopus ID [56578474900](https://orcid.org/0000-0001-5657-8474);

Rashit G. Galin, Scopus ID [7004133681](https://orcid.org/0000-0001-7004-1336);

Vladimir E. Zhivulin, Scopus ID [57044766800](https://orcid.org/0000-0001-5704-4766).

Websites:

Chelyabinsk State University, <https://www.csu.ru/>;

South Ural State University, <https://www.susu.ru/ru>.

References

- Marder AR. The metallurgy of zinc-coated steel. *Prog Mater Sci.* 2000;45(3):191–271. doi:[10.1016/S0079-6425\(98\)00006-1](https://doi.org/10.1016/S0079-6425(98)00006-1)
- Zhang XG. Corrosion and electrochemistry of zinc. New York: Springer Science & Business Media; 2013. 474 p.
- Zhang XG, Leygraf C, Wallinder IO. Atmospheric corrosion of Galfan coatings on steel in chloride-rich environments. *Corros Sci.* 2013;73:62–71. doi:[10.1016/j.corsci.2013.03.025](https://doi.org/10.1016/j.corsci.2013.03.025)
- Duchoslav J, Steinberger R, Arndt M, Keppert T, Luckeneder G, Stellnberger KH, Hagler J, Angeli G, Riener CK, Stifter D. Evolution of the surface chemistry of hot dip galvanized Zn–Mg–Al and Zn coatings on steel during short term exposure to sodium chloride containing environments. *Corros Sci.* 2015;91:311–320. doi:[10.1016/j.corsci.2014.11.033](https://doi.org/10.1016/j.corsci.2014.11.033)
- Zhang XG, Wallinder IO, Leygraf C. Atmospheric corrosion of Zn–Al coatings in a simulated automotive environment. *Surf Eng.* 2017;34(9):1–8. doi:[10.1080/02670844.2017.1305658](https://doi.org/10.1080/02670844.2017.1305658)
- Peng S, Xie SK, Lu JT, Zhang LC. Surface characteristics and corrosion resistance of spangle on hot-dip galvanized coating. *J Alloys Compd.* 2017;728:1002–1008. doi:[10.1016/j.jallcom.2017.09.091](https://doi.org/10.1016/j.jallcom.2017.09.091)
- Zhang XG. Galvanic corrosion of zinc and its alloys. *J Electrochem Soc.* 1996;143:1472–1484. doi:[10.1149/1.1836662](https://doi.org/10.1149/1.1836662)
- Neufeld AK, Cole IS, Bond AM, Furman SA. The initiation mechanism of corrosion of zinc by sodium chloride particle deposition. *Corros Sci.* 2002;44:555–572. doi:[10.1016/S0010-938X\(01\)00056-7](https://doi.org/10.1016/S0010-938X(01)00056-7)
- Prosek T, Hagström J, Persson D, Fuertes N, Lindberg F, Chocholatý O, Taxén C, Šerák J, Thierry D. Effect of the microstructure of Zn–Al and Zn–Al–Mg model alloys on corrosion stability. *Corros Sci.* 2016;110:71–81. doi:[10.1016/j.corsci.2016.04.022](https://doi.org/10.1016/j.corsci.2016.04.022)
- Volovitch P, Vu TN, Allély C, Abdel Aal A, Ogle K. Understanding corrosion via corrosion product characterization: II. Role of alloying elements in improving the corrosion resistance of Zn–Al–Mg coatings on steel. *Corros Sci.* 2011;53(8):2437–2445. doi:[10.1016/j.corsci.2011.03.016](https://doi.org/10.1016/j.corsci.2011.03.016)

11. Ha HY, Park SJ, Kang JY, Kim HD, Moon MB. Interpretation of the corrosion process of a galvanized coating layer on dual-phase steel. *Corros Sci.* 2011;53(7):2430–2436. doi:[10.1016/j.corsci.2011.04.001](https://doi.org/10.1016/j.corsci.2011.04.001)
12. Natrup F, Graf W. Sherardizing: corrosion protection of steels by zinc diffusion coatings. *Thermochemical Surface Engineering of Steels* – Woodhead Publishing. 2015;62:737–750. doi:[10.1533/9780857096524.5.737](https://doi.org/10.1533/9780857096524.5.737)
13. Zhang FH, et al. The corrosion rules study of aluminizing and sherardized carbon-steel in oilfield wastewater. *J Petrochem Univ.* 2012;25(6):44–47. doi:[10.3969/j.issn.1006-396X.2012.06.011](https://doi.org/10.3969/j.issn.1006-396X.2012.06.011)
14. Ataiwi AH, Al-Shalchy SI, Mahdi GA. Characterization of Sherardized Low Carbon Steel Used in Oil Pipelines Coated with Polymer Blends Layers: Part (A). *Eng Technol J* [Internet]. 2015 [cited 2022];33(4):855–867. English. Available from: <https://www.iasj.net/iasj/download/ddbd7513372e3f86>.
15. Galin RG, inventor. Modifitsirovanny poroshok tsinka. Russian Federation patent RU 2170643. 2001 July 20. Russian.
16. Biryukov AI, Zakharyevich DA, Galin RG, Devyaterikova N, Scherbakov I. Corrosion resistance of thermal diffusion zinc coatings of PNTZ in oilfield environments. *EDP Sci.* 2019; 121:02005. doi:[10.1051/e3sconf/201912102005](https://doi.org/10.1051/e3sconf/201912102005)
17. Galin RG, Zakharyevich DA, Rushchits SV. Formation and structure of diffusional zinc coatings formed in nanocrystallized zinc powders. *Materials Science Forum.* Trans Tech Publications Ltd. 2016;870:404–408. doi:[10.4028/www.scientific.net/MSF.870.404](https://doi.org/10.4028/www.scientific.net/MSF.870.404)
18. Galin RG, Shaburova NA, Zakharyevich DA. Thermal Diffusion Galvanizing in Ferriferous Zinc Powder. *Materials Science Forum.* Trans Tech Publications Ltd. 2016;870:129–134. doi:[10.4028/www.scientific.net/MSF.870.129](https://doi.org/10.4028/www.scientific.net/MSF.870.129)
19. Biryukov AI, Galin RG, Zakharyevich DA, Wassilkowska AV, Batmanova TV. The effect of the chemical composition of intermetallic phases on the corrosion of thermal diffusion zinc coatings. *Surface Coat Technol.* 2019;372:166–172. doi:[10.1016/j.surfcoat.2019.05.029](https://doi.org/10.1016/j.surfcoat.2019.05.029)
20. Biryukov AI, Galin RG, Zakharyevich DA, Wassilkowska A, Kolesnikov AV, Batmanova TV. A layer-by-layer analysis of the corrosion properties of diffusion zinc coatings. *Arch Metall Mater.* 2020;65:99–102. doi:[10.24425/amm.2019.131101](https://doi.org/10.24425/amm.2019.131101)
21. Tufanov DG. *Korozionnaya stoykost nerzhavayushchikh staley, splavov i chistyx metallov* [Corrosion resistance of stainless steels, alloys and pure metals]. Moscow: Metallurgy; 1982. 352 p. Russian.
22. Wallinder IO, Leygraf C. A critical review on corrosion and runoff from zinc and zinc-based alloys in atmospheric environments. *Corros.* 2017;73(9):1060–1077. doi:[10.5006/2458](https://doi.org/10.5006/2458)
23. Lindström R, Svensson JE, Johansson LG. The atmospheric corrosion of zinc in the presence of NaCl the influence of carbon dioxide and temperature. *J Electrochem Soc.* 2000;147(5):1751–1757. doi:[10.1149/1.1393429](https://doi.org/10.1149/1.1393429)
24. Ooij WJ, Sabata A. Under-vehicle corrosion testing of primed zinc and zinc alloy-coated steels. *Corros.* 1990;46(2):162–171. doi:[10.5006/1.3585083](https://doi.org/10.5006/1.3585083)
25. Sagiya M, Hiraya A. Analysis of initial oxide films formed on zinc and zinc-iron alloy coatings. *Zairyo-to-Kankyo.* 1993;42(11):721–727. doi:[10.3323/jcorr1991.42.721](https://doi.org/10.3323/jcorr1991.42.721)
26. Biryukov AI, Galin RG, Zakharyevich DA, Tronov AP. Formation and structure of simoncolleite on the surface of thermal diffusion zinc coatings in chloride-containing media. *Corrosion: Protection of metals and physical chemistry of surfaces* [Internet]. 2016[cited 2022];9:28–33. Russian. Available from: <https://www.elibrary.ru/item.asp?id=27703190>
27. Tanaka H, Fujioka A, Futouy A, Kandori K, Ishikawa T. Synthesis and characterization of layered zinc hydroxychlorides. *J Solid State Chem.* 2007;180(7):2061–2066. doi:[10.1016/j.jssc.2007.05.001](https://doi.org/10.1016/j.jssc.2007.05.001)
28. Tanaka H, et al. Role of zinc compounds on the formation, morphology, and adsorption characteristics of β -FeOOH rusts. *Corros Sci.* 2010;52(9):2973–2978. doi:[10.1016/j.corsci.2010.05.010](https://doi.org/10.1016/j.corsci.2010.05.010)